A molecular dynamics and microporomechanics study on the mechanical properties of major constituents of hydrated cement

A. Al-Ostaz [*], W. Wu, A.H.-D. Cheng, C.R. Song

Department of Civil Engineering, University of Mississippi, 203 Carrier Hall, University, MS 38677, USA

ARTICLE INFO

ABSTRACT

Cement paste is the matrix material for concrete and cement based composites. This paper presents a molecular dynamics (MD) method for estimating mechanical properties of hydrated cement major constituents: calcium–silicate–hydrate (C–S–H) structurally related tobermorite 14 Å and jennite, and calcium hydroxide (CH). Microporomechanics technique is used to calculate properties of two types of C–S–H, namely, low density (LD) and high density (HD) C–S–H gels. Simulation results reported by the authors were compared with existing computational and experimental values. This research is intended to give a general step to study the complicated cement hydrated products from a multiscale view.

© 2010 Elsevier Ltd. All rights reserved.

1. Introduction

Cement is one of the most used materials in earth. The US annual consumption of cement reached a record high of 128 million metric tons per year in 2005 and is expected to hit 183 million metric tons per year by 2030 [1]. Since cement is usually produced at high temperature, its production results in high carbon dioxide (CO_2) emission. Cement production accounts for an estimated 5–10% of the world's CO_2 emission, one of the primary green house contributors to global warming. It has been believed that durability and strength of concrete is due to binding properties of cement. However, researchers at Massachusetts Institute of Technology, reported that strength and durability of concrete lies in the organization of cement nanoparticle [2,3]. This discovery can lead to major reduction in carbon dioxide emission during manufacturing. If engineers can reduce CO_2 emission by 10%, that would accomplish one-fifth of the Kyoto Protocol goal of 5.2% reduction of CO_2 emission. Therefore, it is important to take research a step deeper into understanding the relationship between cement products (including cement itself and its hydrated products) properties and their nano structure, which may help to find a possible replacement for the calcium in cement powder, or more realistically to further improve the performance of concrete dramatically, thus the reduction of use of cement may be indirectly achieved. This work reflects the effort to study the cement hydrated products, namely, hydrated cement paste, which is the matrix material for regular concrete and cement based composites.

Different cement hydration products are formed when Portland cement is dispersed in water, calcium silicate hydrate (C–S–H), makes up 50–60% of the volume of solids in completely hydrated cement paste. Crystal structures of C–S–H are closely related to mineral crystals of tobermorite 14 Å and jennite. Calcium hydroxide (CH) crystal (also called portlandite) constitutes 20–25% of volume of solids in the hydrated paste. Other components of hydrated cement paste include calcium sulfoaluminate, unhydrated clinker grains and voids [4]. The dimension of typical hydration products of cement is roughly between 1 and 100 nm, which meets one of the requirements of the definition of nanotechnology proposed by Ratner and coworkers [5,6]. Nanotechnology research and development includes manipulation under control of the nanoscale structures and their integration into larger material components, systems and architectures according to the definition of National Nanotechnology Initiative [7]. Essential in nanotechnology is to have a direct control of matter either between two nano-objects, or between a micro (or macro) object and a nano-object. Therefore, one can use nanomechanics to study mechanical behavior of such material. In this paper, we employ molecular dynamics method to estimate mechanical properties of major constituent materials of hydrated cement.

In this paper, first nano-mechanical properties of cement hydrates are calculated using molecular dynamics technique. Then micro-mechanical properties of low density (LD) and high density (HD) C–S–H gels are estimated using microporomechanics techniques. Two critical issues in MD simulation: choice of force fields and size of the simulating supercell are addressed in this study. This paper and the authors' related work [8–10] intend to set part of the frameworks for correlating concrete mechanical properties to structure of the nanoparticles (such as C–S–H) in concrete.

* Corresponding author. Tel.: +1 662 915 5364; fax: +1 662 915 5523.
E-mail address: alostaz@olemiss.edu (A. Al-Ostaz).

2. Nanostructure of hydrated cement

Among the major constituents of hydrated cement paste, C–S–H is no doubt the most important and complicated constituent. The revealing of C–S–H and cement gel structure began from the milestone work done by Powers and Brownyard [11–13], they proposed a colloidal and gel-like C–S–H model as shown in [11]. According to Powers, the cement gel contains colloidal C–S–H, and noncolloidal calcium hydroxide (CH). The gel particles were once regarded as spheres, later were changed to be platy, or ribbonlike fibers. The porosity in the Powers gel model was estimated to be 28%. Recently Tennis and Jennings [14–16] published a series of paper on a widely accepted C–S–H colloidal model that is shown in Fig. 1. In this model, two types C–S–H are considered: low density (LD) and high density (HD) cement gels which have 37% and 24% gel porosity, respectively. Both LD and HD C–S–H are formed by the basic building block 'Globules' which has a dimension of 5.6 nm and 18% nanoporosity filled by structural water. Gel porosities of C–S–H and nanoporosity of globules are intrinsic properties of concrete, which means they keep the same in any types of C–S–H. Nevertheless the volumetric proportion of LD C–S–H and HD C–S–H changes from one cement paste to another depending on water cement ratio. In the development of microstructure of cement, HD C–S–H is, usually, formed around residual cement clinkers while CH is, generally, formed in between LD C–S–H and adjacent to macropores [17].

Although Jennings model displays a clear picture of the microstructure of C–S–H gel, it does not confirm the crystal structure C–S–H solids. This raises a question of what will be a good prediction of the nature of C–S–H solids that may be used in Jennings gel model. The first model to answer this question was proposed by Taylor [18,19] in 1986. Taylor's model is called T/J model which claimed that C–S–H had a disordered layer structure where most of the layers were structurally imperfect jennite, the rest were structural related 14 Å (1.4 nm) tobermorite. Another model was given by Richardson and Groves in 1992 and 1993 [20,21] and called T/CH model. The T/CH model treated C–S–H as a tobermorite-'solid solution' calcium hydroxide, which means tobermorite-like structure interstratified with layers of calcium hydroxide [22]. Since Richardson and Groves' model is a constitutional model in nature, we adopt Taylor's T/J C–S–H gel structure model in our simulation. Unfortunately there is currently no literature with detailed real C–S–H structure reported. The exact nanostructure of the C–S–H disordered layer structure has not yet been decrypted, while structure-related crystals tobermorite 14 Å and jennite are recently given by Bonaccorsi et al. [23,24]. It is necessary to point out that recent research [25] shows the formula for actual C–S–H is $(CaO)_{1.7}(SiO_2)(H_2O)_{1.8}$ which has a Ca/Si ratio 1.7. The poorly crystalline or amorphous calcium silicate hydrates, which varies in Ca/Si ratio from the value from 0.83 (i.e. for tobermorite 14) to as high as about 1.5 (for jennite) [24]. Although tobermorite and jennite do not have exactly the same structure of real C–S–H, it is a common practice for cement and concrete researchers to use them to study C–S–H at this time. The authors believe the same approach reported in this paper can be utilized to obtain the mechanical properties once the real and detailed atomic structure of C–S–H is revealed in the future.

Manzano et al. [26] simulated mechanical properties of crystalline C–S–H gel compounds by lattice dynamics method. The Young's moduli they calculated were 91 GPa for tobermorite 14 Å and 66 GPa for jennite.

It is relatively difficult to perform direct mechanical testing to measure the properties of the solid C–S–H and only limited works is reported in the literature. Ulm et al. [17,27] used nanoindentation technique and micorporomechanics theories to calculate the solid phase elastic modulus indirectly.

In this paper, molecular dynamics approach using commercially available Materials Studio software [28] is used to obtain properties of jennite and tobermorite 14 Å. Crystal structure of 14 Å tobermorite presented follows the latest finding by Bonaccorsi et al. [23]. Tobermorite 14 Å has the chemical formula $Ca_5Si_6O_{16}(OH)_2 \cdot 7H_2O$. The most distinguished characteristic of 14 Å tobermorite is that it has a typical layer structure as shown in Fig. 2. The water molecular is modeled between calcium polyhedra layers. The crystal structure is formed by a central sheet with CaO_2 stoichiometry, connected on both sides to silicate chains with periodicity of three tetrahedra (dreierketten, or wollastonite-like chains). The space in between layers contains a larger amount of H_2O molecules. It is expected to have anisotropic material properties from MD computation due to the nature of the crystal structure. The crystal structure of jennite which as a Ca/Si ratio of 1.5 (Fig. 3) is built up by the three modules: ribbons of edge-sharing calcium octahedra, silicate chains of wollastonite-type, and additional calcium octahedra. Study [29] shows that at later age, jennite-type C–S–H become dominate.

Except for major hydrated cement product C–S–H, calcium hydroxide (CH, also called portlandite) constitutes 20–25% volume of solids in the cement paste. CH usually forms much larger crystal with hexagonal-prism or platy shape morphology, as shown in Fig. 4.

3. Methods and results

3.1. Molecular dynamics simulation of C–S–H solid and CH

Molecular dynamics simulation method had been used to obtain the mechanical properties of solid C–S–H, and CH. The same
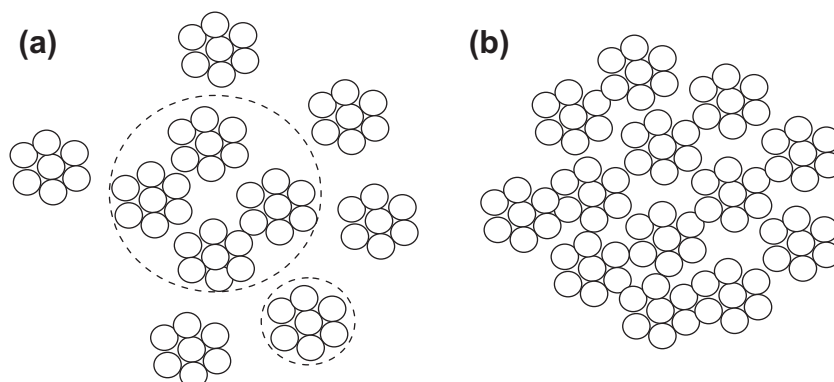

Fig. 1. Two types of C–S–H (a) LD and (b) HD.

(a)

silicon tetrahedra chain   calcium polyhedra   calcium polyhedra layer
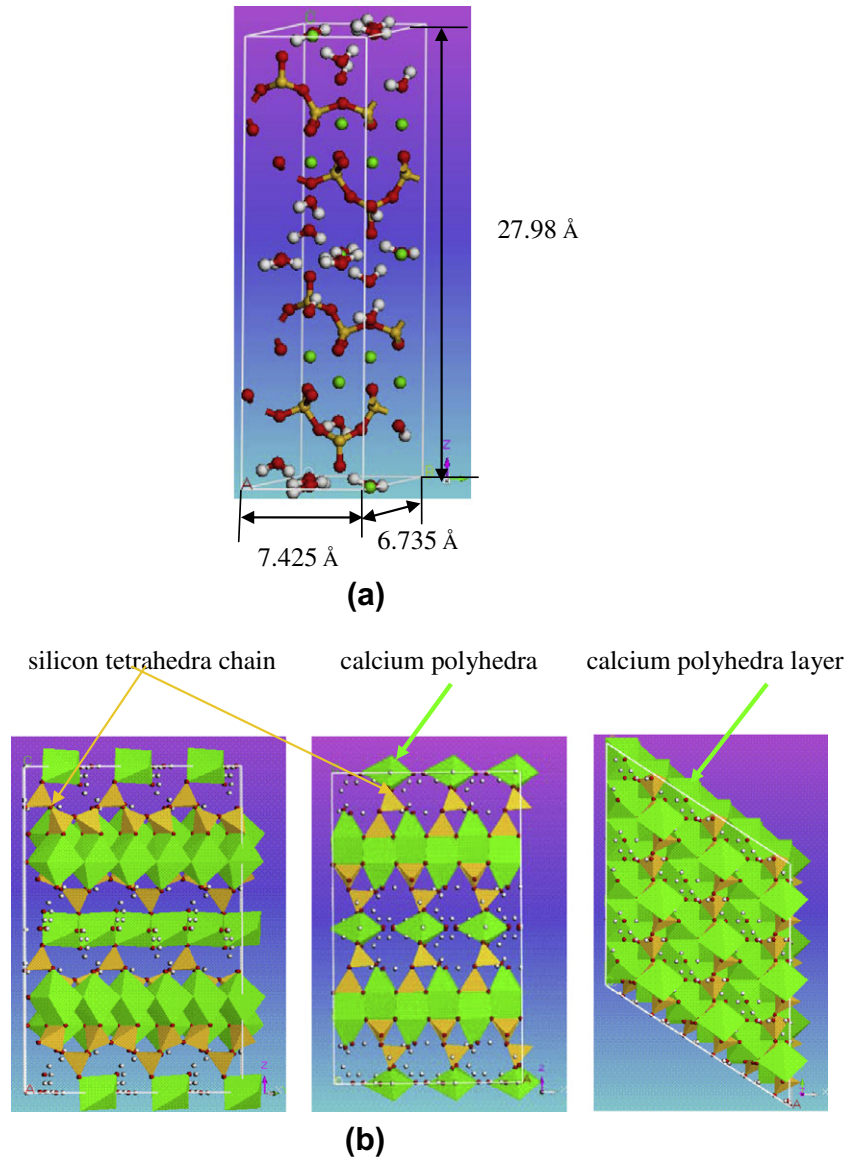
(b)

Fig. 2. Unit cell of crystal 14 Å tobermorite (a) perspective (b) different views of a supercell structure of 14 Å tobermorite (red – oxygen O; green – calcium Ca; orange – silica Si; white – hydrogen H). (For interpretation of the references to colour in this figure legend, the reader is referred to the web version of this article.)
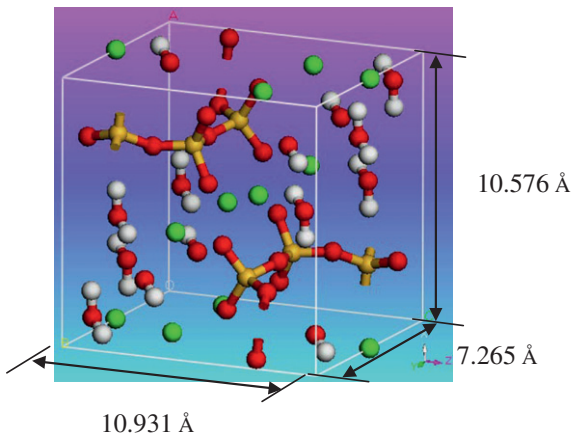

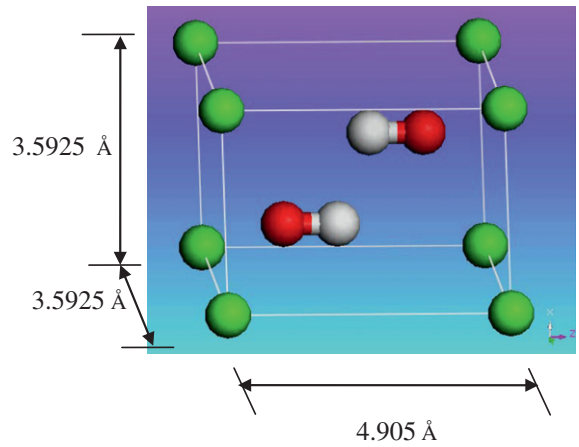**Fig. 3.** Unit cell of crystal jennite perspective view.

Fig. 4. Unit cell of crystal calcium hydroxide.

method was adopted by manzano, Pellenq et al. [30,31] in the study of some aspects of C–S–H. Molecular dynamics is one of the modeling schemes of molecular mechanics, which directly calculate the potential energy surface by solving classical Newton's equation of motion:

$$-\frac{dE}{dR} = m\frac{d^2R}{dt^2} \tag{1}$$

where E is potential energy, R represents position of the nuclei, m is mass and t is time. The solution of Newton's equation in MD needs an empirical fit to the potential energy surface, which is often called a forcefield [32].

Choosing proper force fields is a crucial step in MD simulation. A forcefield is the average description of the existing interactions among various atoms in a molecule or a group of molecules which has a set of functions and parameters in molecular mechanics and molecular dynamics [33]. Unfortunately there is no guidance to choose a right forcefield for hydrated cement materials simulation, therefore, it is desirable to try different available forcefields. Two forcefields, Condensed-phase Optimized Molecular Potentials for Atomic Simulation Studies (COMPASS) [34] and Universal (UFF) [35], were adopted in this study. The potential energy functional forms for the above two force fields were given in Eqs. (2) and (3), respectively. COMPASS forcefield is a high quality general ab initio forcefield, which has been widely used in simulations of liquids, crystals, and polymers.

The COMPASS covers most common organic molecules, polymers, small gas molecules, inorganic materials including metals (Al, Fe, Mg, etc.), metal halides (Ca++, Fe−, etc.), Silica/Aluminosilicates (SiO_2, AlO_2) and metal oxides (CaO, Al_2O_3, SiO_2, etc.) [36], which is applicable to this study. The potential energy for COMPASS can be expressed in the form [33] of

$$
\begin{aligned}
E_{total} =& \sum_b [K_2(b-b_0)^2 + K_3(b-b_0)^3 + K_4(b-b_0)^4] \\
&+ \sum_\theta [K_{2\theta}(\theta-\theta_0)^2 + K_{3\theta}(\theta-\theta_0)^3 + K_{4\theta}(\theta-\theta_0)^4] \\
&+ \sum_\phi [K_{1\phi}(1-\cos\phi) + K_{2\phi}(1-\cos 2\phi) + K_{3\phi}(1 \\
&- \cos 3\phi)] + \sum_\chi K_{2\chi}(\chi-\chi_0)^2 + \sum_{b,\theta} K_{b\theta}(b-b_0)(\theta-\theta_0) \\
&+ \sum_{b,\phi} (b-b_0)[K_{1b}\cos\phi + K_{2b}\cos 2\phi + K_{3b}\cos 3\phi] \\
&+ \sum_{\theta,\phi} (\theta-\theta_0)[K_{1\theta\phi}\cos\phi + K_{2\theta\phi}\cos 2\phi + K_{3\theta\phi}\cos 3\phi] \\
&+ \sum_{b,\theta} (\theta'-\theta_0')(\theta-\theta_0) + \sum_{\theta,\phi} K_{\theta\phi}(\theta'-\theta_0')(\theta-\theta_0)\cos\phi \\
&+ \sum_{i,j} \frac{q_iq_je}{r_{ij}} + \sum_{i,j} \varepsilon_{ij}\left[2\left(\frac{r_{ij}^0}{r_{ij}}\right)^9 - 3\left(\frac{r_{ij}^0}{r_{ij}}\right)^6\right]
\end{aligned} \tag{2}
$$

where the first 10 terms are valence terms. The first through fourth terms represent the energy associated with bond, angle, torsion, and out-of-plane internal coordinates respectively. The fifth to eighth terms represent the energies of cross-coupled internal coordinates which are important for calculating the vibration frequencies and structural variations associated with conformational changes. The last two terms represent non-bond interaction between atoms separated by two or more intervening atoms, or belonging to different molecules. The second-to-last term is the Coloumb potential that represents electrostatic interactions. The last term of Eq. (2), that is the Lenard-Johns 9-6 (LJ 9-6) potential, represents the van der Waals interaction. The valence parameters and atomic partial charges were derived by fitting to ab initio data, and the van der Waals (vdW) parameters were derived by conducting MD simulations of molecular liquids and fitting the simulated cohesive energies and equilibrium densities to experimental data.

The potential energy of UFF [35] is expressed as:

$$
\begin{aligned}
E_{total}^{UFF} =& E_R + E_\theta + E_\phi + E_\omega + E_{vdW} + E_{el} \\
=& \frac{1}{2}K_{ij}(r-r_{ij})^2 + K_{ijk}\sum_{n=0}^{m} C_n\cos n\theta + K_{ijkl}\sum_{n=0}^{m} C_n\cos n\phi_{ijkl} \\
&+ K_{ijkl}(C_0 + C_1\cos\omega_{ijkl} + C_2\cos 2\omega_{ijkl}) \\
&+ D_{ij}\left\{-2\left[\frac{x_{ij}}{x}\right]^6 + \left[\frac{x_{ij}}{x}\right]^{12}\right\} + 332.0637\left(\frac{Q_iQ_j}{\varepsilon R_{ij}}\right)
\end{aligned} \tag{3}
$$

where K_{ij}, K_{ijk}, K_{ijkl} are force constants, θ is the periodic angle in Fourier expansion, C_n is expansion coefficient defined by the natural bond angle θ_0, r is bond length, r_0 is the natural bond length, ω_{ijkl} is the angle between the il axis and ijk plane, D_{ij} is the well depth, x_{ij} is the van der Waals bond length. One may notice the angle bending, torsions and inversions are all described by cosine-Fourier expansion terms. The expression does not contain crossterms as appeared in COMPASS force field potential energy. The parameters used to generate the UFF include a set of hybridization dependent atomic bond radii, a set of hybridization angels, van der Waals as shown in Table 1 in [35]. The UFF includes a parameter generator that calculates forcefield parameters by combining these atomic parameters.

The most distinguishing advantage of UFF lies in the fact that it covers a full periodic table, which means when COMPASS fails to work on some crystals, one can always switch to UFF. UFF is only incorporated in Forcite in Materials Studio while COMPASS is available in both Discover and Forcite. Discover and Forcite are two molecular mechanics tools in Materials Studio.

It is necessary to minimize the structures and obtain energy-optimized structures before performing dynamics. For systems with less than 200 atoms, we use a smart minimization method which combines a steepest descent, conjugate gradient and Newton–Raphson method, starting with the steepest descent method, followed by the conjugate gradient method and ends with a Newton–Raphson method. Newton–Raphson method is replaced with conjugate gradients method when dealing with larger systems. The cutoff distance in all the simulations is 12.50 Å. Ewald summation method is used to determine non-bond (van der Waals interactions and coulomb electrostatic) energies. Energy minimized models were used as initial structures for molecular dynamics simulations that were performed as NPT canonical ensembles at P = 0.001 GPa (air pressure) and T = 298 K (room temperature). Choice of NPT ensemble is based on the works [37,38]. Andersen thermostat temperature controlling method and Parrinello barostat pressure controlling scheme were applied in the Discover runs. The Nosé thermostat temperature controlling method and Berendsen barostat pressure controlling scheme were employed in the Forcite simulations. Another important parameter is time step. The criterion for choosing time step is the step should be small compared to the average time between molecules collisions. Usually the time step should be approximately one tenth of the shortest period of motion of molecules [39]. 1 fs (femtosecond, 10^{-15} s) is chosen in this work following [35,38]. Depending on the number of atoms in the system, the dynamics time used in this research ranges between 100 ps (picosecond, 10^{-12} s) and 400 ps.
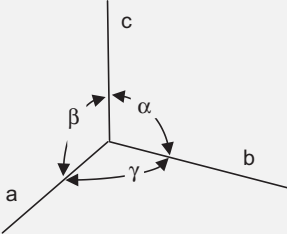
The dynamics simulations were carried out in two stages, equilibration and data collection. In the first stage, the system will be brought to the most probable configuration consistent with the target temperature and pressure. To ensure thermodynamic equilibrium, thermodynamics quantities such as energy and temperature, versus time were constantly monitor. When equilibration has been achieved, these quantities fluctuate around their averages, which remain constant over time [32].

Table 1
Molecular mechanics simulation condition.

Name of condition	Conditions used in this study		
	Tobermorite 14 Å	Jennite	CH
Cell size (Å)	6.735 × 7.425 × 27.987	10.576 × 7.265 × 10.931	3.5925 × 3.5925 × 4.905
No. of atoms	124	69	5
Molecular tools	Discover/Forcite	Discover/Forcite	Discover/Forcite
Force fields	Compass, UFF	Compass	Compass
MD ensemble	NPT	NPT	NPT
Temperature (°C)	25	25	25
Temperature control (GPa)	Andersen/Nose	Andersen/Nose	Andersen/Nose
Pressure	0.001	0.001	0.001
Pressure control	Parrinello/Berendsen	Parrinello/Berendsen	Parrinello/Berendsen
Time step (fs)	1	1	1
Dynamics time (ps)	System with number of atoms N > 1000, 300 ps were used, N > 2000, 400 ps were used, minimum 100 ps were used		

fs: femtosecond; ps: picosecond; NPT: N-constant number of particles in the simulation system; P: constant pressure; T: constant temperature.

Table 2
Cell parameters of crystal tobermorite 14 Å, jennite and CH.

Crystal system	Tobermorite	Jennite	CH
Lattice type	Monoclinic	Triclinic	Trigonal
a (Å)	6.735	10.576	3.5925
b (Å)	7.425	7.265	3.5925
c (Å)	27.987	10.931	4.90
α (°)	90	101.30	90
β (°)	90	96.98	90
γ (°)	123.25	109.65	120
Notation			

After dynamics simulation has been performed, we analyze the resulting deformed molecular structure to determine elastic constants. Elastic constants of the final atomic configuration are computed using the static approach suggested by Theodorou and Suter [40]. The elastic constants in this approach are defined as:

$$C_{lmnk} = \frac{\partial \sigma_{lm}}{\partial \varepsilon_{nk}}\bigg|_{T,\varepsilon_{nk}} = \frac{1}{V_o}\frac{\partial^2 A}{\partial \varepsilon_{lm}\partial \varepsilon_{nk}}\bigg|_{T,\varepsilon_{lm},\varepsilon_{nk}} \qquad (4)$$

where C is stiffness constant, σ is the stress component, ε is the strain component, A denotes the Helmholtz free energy, and V_o is the volume of the simulation cell in the undeformed configuration. We calculate the corresponding isotropic polycrystalline elastic moduli based on the corresponding single-crystal elastic constants by Voigt–Reuss–Hill (VRH) approximation [41,42]. Molecular

mechanics simulation conditions and basic input information regarding the structures are shown in Tables 1 and 2, respectively.

The mechanical properties obtained from MD simulation for tobermorite 14 Å, jennite and CH, are summarized in Tables 3–5, respectively. The Young's moduli of tobermorite 14 Å, jennite and CH calculated by MD in this study are 50.6 GPa, 66.9 GPa and 51.5 GPa, while the values given in the current literature are: 91 GPa, 66 GPa and 42.3 GPa. Compared to the values existing in the literature, MD yields fair results for jennite and CH. There is a difference for tobermorite 14 Å, the average Young's modulus reported in this work is about 44% less than the lattice dynamics calculation result. As for the CH simulation results shown in Table 5, one may notice that Discover-COMPASS combination yields unreasonable results which are either too high or too low compared to literature values. Forcite-COMPASS with unit simulation cell gives result most close to the value reported in [44]. The variation of current MD simulating results raises a concern about the choice of force field, simulation supercell size, and molecular mechanics tool (in this study, either Discover or Forcite).

3.2. Micropormechanics effective properties calculation of LD and HD C–S–H

C–S–H gel is a porous material with 37% (LD) and 24% (HD) porosity. Microporomechanics is a very useful tool to study the

Table 4
Molecular simulation results of jennite.

Supercell properties	1a × 1b × 1c		2a × 2b × 2c	Literature values [26]
	F–C	D–C	F–C	
E (GPa)	44.1	82.2	66.9	66
v	0.28	0.33	0.34	0.24
K (GPa)	33.3	78.4	69	43
G (GPa)	17.2	31.0	25	26

F: Forcite, D: Discover, U: UFF, C: COMPASS forcefield.

Table 3
Molecular simulation results of tobermorite 14 Å.

Supercell properties	1a × 1b × 1c[a]		2a × 2b × 2c	3a × 3b × 3c	Literature values [26]
MD tools & forcefields	F–U	D–C	D–C	D–C	
E (GPa)	42.94	43.01	51.4	49.82	91
v	0.29	0.343	0.328	0.343	0.17
K (GPa)	33.4	45.68	49.79	52.89	46.0
G (GPa)	16.7	16.01	19.35	18.55	39

F: Forcite, D: Discover, U: UFF; C: COMPASS forcefield.
[a] a, b, c are dimensions of the unit cell of the crystal structure.

Table 5
Molecular simulation results of CH.

Supercell properties	1a × 1b × 1c		2a × 2b × 2c		3a × 3b × 3c		Literature values [44]
MD tools & forcefields	D–C	F–C	D–C	F–C	D–C	F–C	
E (GPa)	152	51.5	195	74.5	22.4	65.2	42.3
v	0.16	0.31	0.31	0.28	0.45	0.3	0.324
K (GPa)	180.5	44.6	174.6	56.9	77.3	55.5	40
G (GPa)	109.3	19.7	74.3	29.1	7.7	25	16

F: Forcite, D: Discover, U: UFF, C: COMPASS forcefield.

Table 6
Computation of LD and HD mechanical properties.

C–S–H	Porosity ϕ_0 (%)	K_s (GPa)	G_s (GPa)	E (GPa)	E_{ref} (GPa)	v	v_{ref}
LD	37	25	69	30.8	21.7 [43] 23.4 [45]	0.29	0.24 [43]
HD	24	25	69	41	29.4 [43] 31.4 [45]	0.3	0.24 [43]

E_{ref}: reference values for modulus of elasticity. v_{ref}: reference values for Poisson's ratio.

mechanics and physics of multiphase porous materials [43]. According to Mehta and Monteiro [4], the poroelastic properties of LD and HD C–S–H can be derived by:

$$K = G_s \frac{4(1 - \phi_0)}{3\phi_0 + 4(G_s/K_s)} \tag{5}$$

$$G = G_s \frac{(1 - \phi_0)(8G_s + 9K_s)}{6\phi_0(2G_s + K_s) + 8G_s + 9K_s} \tag{6}$$

where K and G are effective bulk and shear moduli, G_s and K_s are shear and bulk modulus of the solids, ϕ_0 is porosity.

Based on Taylor's T/J C–S–H model, the majority of C–S–H solids are jennite type. Therefore, we use mechanical properties of jennite obtained from MD simulations to represent the solid properties needed in Eqs. (5) and (6) to compute effective properties K and G of LD and HD C–S–H. Results are shown in Table 4. LD and HD C–S–H moduli calculated are 30.8 GPa and 41 GPa. From the computed properties of two types of C–S–H shown in Table 4, it is observed that there is a relatively big difference between our obtained values and the ones obtained using nanoindentation test. This may be due to the fact that we use jennite to model C–S–H instead of using its real atomic structure (see Table 6).

4. Conclusions and discussions

This study is an essential step to model concrete as a hierarchical structural composite material [10], which also presents a general idea on part of the procedures for multiscale modeling of hydrated cement paste and cement based composites.

We attempt to use molecular dynamics method to compute the major constituents of hydrated cement. The mechanical properties for CH and jennite are comparable to those reported in the literature. As an initial study of using MD on cement based materials simulation, MD can be a candidate to obtain the mechanical properties of mineral crystals at nanoscale. But the effect of forcefield and supercell size are obvious, namely, the results of hydrated cement depend on the specific forcefield and the simulation supercell size, which are the important issues needed to be addressed in the near future. Another important consideration is that we need a real amorphous structure of C–S–H which has not yet been fully understood.

Based on the molecular dynamics simulation results of C–S–H structural related crystals, we apply microporomechanics to the computation of mechanical properties of larger scale LD and HD C–S–H, which are two constituent materials in authors' proposed hydrated cement composite model reported in paper "concrete as a hierarchical structural composite material" [10].

References

[1] Sullivan E. Long-term cement consumption outlook, PCA the monitor forecast report, January 31; 2008.
[2] Brehm D, editor. Nanoengineered concrete could cut carbon dioxide emissions. <http://web.mit.edu/newsoffice/2007/concrete.html>.
[3] Brehm D, editor. MIT's Department of civil and environmental engineering brochure on balance: nanoengineered concrete could cut world CO2. Cambridge (MA); 2007.
[4] Mehta PK, Monteiro PJM. Concrete: microstructure, properties, and materials. New York: McGraw Hill; 1993.
[5] Ratner M, Ratner D. Nanotechnology – a gentle introduction to the next big idea. NJ: Prentice Hall; 2002.
[6] Migugel YR de, Porro A, Bartos PJM. In: 2nd international symposium on nanotechnology in construction: NICOM 2, Bilbao, Spain. Bagneux (France): Rilem Publications S.a.r.l.; 2005.
[7] National nanotechnology initiative, what is nanotechnology. <http://www.nano.gov/html/facts/whatIsNano.html>.
[8] Wu W, Al-Ostaz A, Cheng A H-D, Song CR. A molecular dynamics study on the mechanical properties of major constituents of Portland cement. ASCE J. Nanomech & Micromech., in press.
[9] Song CR, Wu W, Al-Ostaz A. Effects of force field in molecular mechanics simulation of geo-materials. In: Proceedings of GeoCongress 2008, ASCE GSP 179, New Orleans, March, 2008. p. 1012–9.
[10] Wu W, Al-Ostaz A, Cheng AH-D, Song CR. Concrete as a hierarchical structural composite material. Int J Multiscale Comput Eng, in press.
[11] Powers TC, Brownyard TL. Studies of the physical properties of hardened Portland cement paste. PCA Bull 1948;22.
[12] Powers TC. The physical structure and engineering properties of concrete. PCA Bull 1958;90:1–26.
[13] Powers TC. Physical properties of cement paste. In: Proceedings of the fourth international symposium on the chemistry of cement. Washington (DC); 1960. p. 577–609.
[14] Tennis PD, Jennings HM. A model for two types of calcium silicate hydrate in the microstructure of Portland cement pastes. Cem Concr Res 2000;30(6): 855–63.
[15] Jennings HM. Colloid model of C–S–H and implications to the problem of creep and shrinkage. Mater Struct 2004;37:59–70 [special issue of concrete science and engineering on pormechanics of cement based materials].
[16] Jennings HM. A model for the microstructure of calcium silicate hydrate in cement paste. Cem Concr Res 2000;30:101–16.
[17] Dormieux L, Ulm F-J, editors. Applied micromechanics of porous materials. CISM courses and lectures. NewYork: Springer Wien; 2005.
[18] Taylor HFW. Proposed structure for calcium silicate hydrate gel. J Am Ceram Soc 1986;69:464–7.
[19] Taylor HFW. Nanostructure of C–S–H: current status. Adv Cem Based Mater 1993;1:38–46.
[20] Richardson IG, Groves GW. Models for the composition and structure of calcium silicate hydrate (C–S–H) gel in hardened tricalcium silicate pastes. Cem Concr Res 1992;22:1001–10.

[21] Richardson IG, Groves GW. The incorporation of minor and trace elements into calcium silicate hydrate (C–S–H) gel in hardened cement pastes. Cem Concr Res 1993;23:131–8.
[22] Richardson IG. Tobemorite/jennite- and tobemorite/calcium hydroxide-based models for the structure of C–S–H: applicability to hardened pastes of tricalcium silicate, β-dicalcium silicate, Portland cement, and blends of Portland cement with blast-kace slag, metakaolin, or silica fume. Cem Concr Res 2004;34:1733–77.
[23] Bonaccorsi E, Merlino S, Kampf AR. The crystal structure of tobermorite 14 A (plombierite), a C–S–H phase. J Am Ceram Soc 2005;88(3):505–12.
[24] Bonaccorsi E, Merlino S, Taylor HFW. The crystal structure of jennite, $Ca_9Si_6O_{18}(OH)_6 \cdot 8H_2O$. Cem Concr Res 2004;34:1481–8.
[25] Allen AJ, Thomas JJ, Jennings HM. Composition and density of nanoscale calcium–silicate–hydrate in cement. Nat Mater 2007;6:311–6.
[26] Manzano H, Dolado JS, Guerrero A, Ayuela A. Mechanical properties of crystalline calcium–silicate–hydrates: comparison with cementitious C–S–H gels. Phys Stat Sol (a) 2007;204(6):1775–80.
[27] Ulm F-J, Constantinides G, Heukamp FH. Is concrete a poromechanics material? – a multiscale investigation of poroelastic properties. Mater Struct/Concr Sci Eng 2004;37:43–58.
[28] Accelrys Inc. Materials studio 4.2 software. San Diego (CA); 2007.
[29] Taylor HFW. Cement chemistry. 2nd ed. London: Thomas Telford Ltd.; 1997.
[30] Manzano H, Dolado JS, Griebel M, Hamaekers J. A molecular dynamics study of the aluminosilicate chains structure in Al-rich calcium silicate hydrated (C–S–H) gels. Phys Stat Sol (a) 2008;205(6):1324–9.
[31] Pellenq RJ-M, Lequeux N, Van Damme H. Engineering the bonding scheme in C–S–H: the iono-covalent framework. Cem Concr Res 2008;3:159–74.
[32] Accelrys Inc. Materials studio 4.2 Manual, San Diego (CA); 2007.
[33] Al-Ostaz A, Pal G, Mantena PR, Cheng A. Molecular dynamics simulation of SWCNT–polymer nanocomposite and its constituents. J Mater Sci 2008;43:164–73.
[34] Sun H. COMPASS: an ab initio forcefield optimized for condensed-phase application-overview with details on alkane and benzene compounds. J Phys Chem 1998;B102:7338–64.
[35] Rappe AK, Casewit CJ, Colwell KS, Goddard III WA, Skiff WM. UFF, a full periodic table force field for molecular mechanics and molecular dynamics simulations. J Am Chem Soc 1992;114(25):10024–35.
[36] The Scripps Research Institute. COMPASS. <http://www.scripps.edu/rc/softwaredocs/msi/cerius45/compass/COMPASSTOC.doc.html>.
[37] Kalinichev AG, Wang J, Kirkpatrick RJ. Molecular dynamics modeling of the structure, dynamics and energetics of mineral–water interfaces: application to cement materials. Cem Concr Res 2007;37(3):337–47.
[38] Cygan RT. Molecular models of hydroxide, oxyhydroxide, and clay phases and the development of a general force field. J Phys Chem B 2004;108:1255–66.
[39] Leach AR. Molecular modeling principles and applications. Essex (England): Addison Wesley Longman Limited; 1996.
[40] Theodorou DN, Suter UW. Atomistic modeling of mechanical properties of polymeric glasses. Macromolecules 1986;19:139–54.
[41] Chung DH, Buessem WR. The Voigt–Reuss–Hill (VRH) approximation and the elastic moduli of polycrystalline ZnO, TiO_2, and Al_2O_3. J Appl Phys 1968;39(6):2777–82.
[42] Hill R. The elastic behavior of a crystalline aggregate. Proc Phys Soc 1952;65:349–54.
[43] Constantinides G, Ulm F-J. The effect of two types of C–S–H on the elasticity of cement-based materials: results from nanoindentation and micromechanical modeling. Cem Concr Res 2004;34:67–80.
[44] Speziale S, Reichmann HJ, Schilling F, Wenk HR, Monteiro PJM. The elastic properties of natural portlandite, $Ca(OH)_2$. In: AGU Fall Meeting 2007. San Francisco, USA, December, 2007.
[45] Zhu W, Huges JJ, Bicanic B, Pearce CJ. Nanoindentation mapping of mechanical properties of cement paste and natural rocks. Mater Charact 2007;58:1189–98.